AIP Advances

Analysis of thermal demagnetization behavior of Nd–Fe–B sintered magnets using magnetic domain observation

Masaaki Takezawa, Soichiro Ikeda, Yuji Morimoto, and Hisayuki Kabashima

Citation: AIP Advances **6**, 056021 (2016); doi: 10.1063/1.4944402
View online: http://dx.doi.org/10.1063/1.4944402
View Table of Contents: http://scitation.aip.org/content/aip/journal/adva/6/5?ver=pdfcov
Published by the AIP Publishing

Analysis of thermal demagnetization behavior of Nd–Fe–B sintered magnets using magnetic domain observation

Masaaki Takezawa,[1,a] Soichiro Ikeda,[1] Yuji Morimoto,[1]
and Hisayuki Kabashima[2]
[1]*Department of Applied Science for Integrated System Engineering, Faculty of Engineering, Kyushu Institute of Technology, 1-1 Sensui-cho, Tobata-ku, Kitakyushu, Fukuoka 804-8550, Japan*
[2]*Mazda Motor Corporation,3-1, Shinchi, Fuchu-cho, Aki-gun Hiroshima 730-8670, Japan*

(Presented 12 January 2016; received 5 November 2015; accepted 12 January 2016; published online 11 March 2016)

We used magnetic domain observation to statistically observe the thermal demagnetization behavior of Nd–Fe–B sintered magnets at elevated temperatures up to 150 °C. Simultaneous magnetization reversal in a hundred adjacent grains occurred at 90 °C because of the magnetic interaction among the grains beyond grain boundaries in the Dysprosium (Dy)-free low-coercivity magnet. Conversely, simultaneous magnetization reversal in a hundred grains did not occur in the Dy-added high-coercivity magnets, and the demagnetizing ratio steadily increased with temperature. Furthermore, the addition of Dy induced high thermal stability by eliminating the simultaneous thermal demagnetization, which was caused by the magnetic interaction among the grains. [http://dx.doi.org/10.1063/1.4944402]

I. INTRODUCTION

Synchronous motors using Nd–Fe–B permanent magnets are widely used for achieving high energy efficiency for hybrid electrical vehicles. Because thermal stability up to a temperature of 200 °C is required for these vehicles, heat-resistant Nd–Fe–B high-coercivity magnets are required. Therefore, for enhancing coercivity, commercially available Nd–Fe–B sintered magnets containing a large amount of the rare metal Dysprosium (Dy) are used.[1,2] However, the low amount of natural reserves of Dy is a crucial resource problem. The reduction and optimization of the Dy content are required for developing a highly efficient motor with a low cost. The purpose of this study was to use magnetic domain observation to observe the thermal demagnetization behavior of Nd–Fe–B magnets depending on the amount of Dy contained in the magnets. We used a Kerr microscope for *in situ* domain observations of high magnetic fields at high temperatures.[3,4] We previously reported through magnetic domain observation that simultaneous magnetization reversal occurred in several grains at elevated temperatures.[5] In this study, with an image-processing technique using a Kerr microscope in a wide observation area, we statistically examined the thermal demagnetization process of Nd–Fe–B sintered magnets uniformly heated by a constant-temperature oven. Consequently, we were able to clarify the relationship between coercivity and the thermal demagnetization process.

II. EXPERIMENTAL PROCEDURES

We observed the magnetic domain of Nd–Fe–B sintered magnets using a Kerr microscope. The intrinsic coercivity of three types of the sample was approximately $\mu_0 H_c$ = 1.25 T, 1.69 T, and

[a]Electronic mail: take@ele.kyutech.ac.jp

2.05 T. Dy was added into two samples with $\mu_0 H_c$ = 1.69 and 2.05 T. The magnets were 7.0 mm thick, 7.0 mm long, and 7.0 mm wide, and the surface at the c-plane of the samples was polished to clearly reveal the domain configuration during the experiments. A thin film of Tantalum (Ta) was deposited by RF sputtering on the surface of the Nd–Fe–B sintered magnets to prevent oxidation. Then, using vacuum evaporation, a thin film of silicon monoxide (SiO) was deposited on the thin film of Ta, which functioned as an antireflection coating. A pulse field of 5 T along the easy axis was used to magnetize all three magnets. The magnetic domains at the center area of these magnets were observed during the thermal demagnetization process. First, the magnetic domain was observed at room temperature (25 °C). Following this, the temperature of the sample, measured by a thermocouple on the sample surface, was increased to 35 °C using a constant-temperature oven, and then, the temperature immediately decreased to room temperature. Next, the temperature was increased to 40 °C and then decreased to room temperature. This procedure was repeated to bring the temperature up to 150 °C in 5 °C increments for each observation, as shown in Fig. 1. To observe the thermal demagnetization in detail, we derived the domain change by subtracting the domain image at one temperature from that at another temperature using a photo-editing application.[6]

III. RESULTS AND DISCUSSION

A. Results of magnetic domain observation

Figure 2 shows domain images of the Dy-free Nd–Fe–B sintered magnet with a coercivity of $\mu_0 H_c$ = 1.25 T. The bright and dark domains are magnetized along the polar directions of the surface in Figs. 2(a) and 2(b). Black regions in domain images are defects caused by oxidation of the rare earth element and polishing. Some demagnetized grains having a multi-domain state were observed in Fig. 2(a) after the magnet was heated to 35 °C. Many demagnetized grains could be observed before heating. The first reversed domains nucleated after the magnet was heated to 35 °C, and the domain structure changed from a single-domain state to a multi-domain state in one grain, as indicated by the solid-line ellipse in Fig. 2(a). After heating at 90 °C, simultaneous magnetization reversal occurred in several adjacent grains beyond the grain boundaries, as indicated by the solid-line ellipse in Fig. 2(b). Figure 2(c) shows the processed domain image indicating the magnetization-reversal area for each temperature at 25 °C increments. We found that simultaneous magnetization reversal in several grains occurred above 75 °C.

Figure 3 shows domain images of the Dy-added Nd–Fe–B sintered magnet with a coercivity of $\mu_0 H_c$ = 1.69 T. Some demagnetized grains could be observed before heating, and the reversed domains nucleated after 55 °C heating. The domain structure changed from a single-domain state to a multi-domain state in the grains, as indicated by the solid-line ellipse in Fig. 3(a). We observed the first magnetization reversal for the magnet with a coercivity of $\mu_0 H_c$ = 1.69 T at 55 °C, which is higher than that for the magnet with a coercivity of $\mu_0 H_c$ = 1.25 T. After heating the magnet to

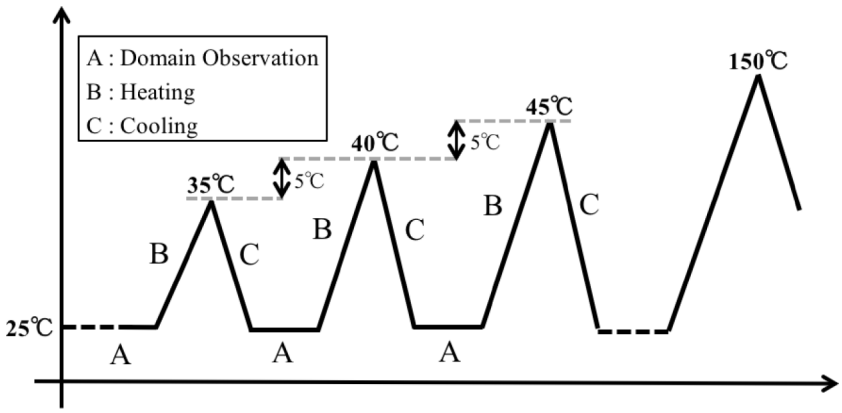

FIG. 1. Flow of the experiment.

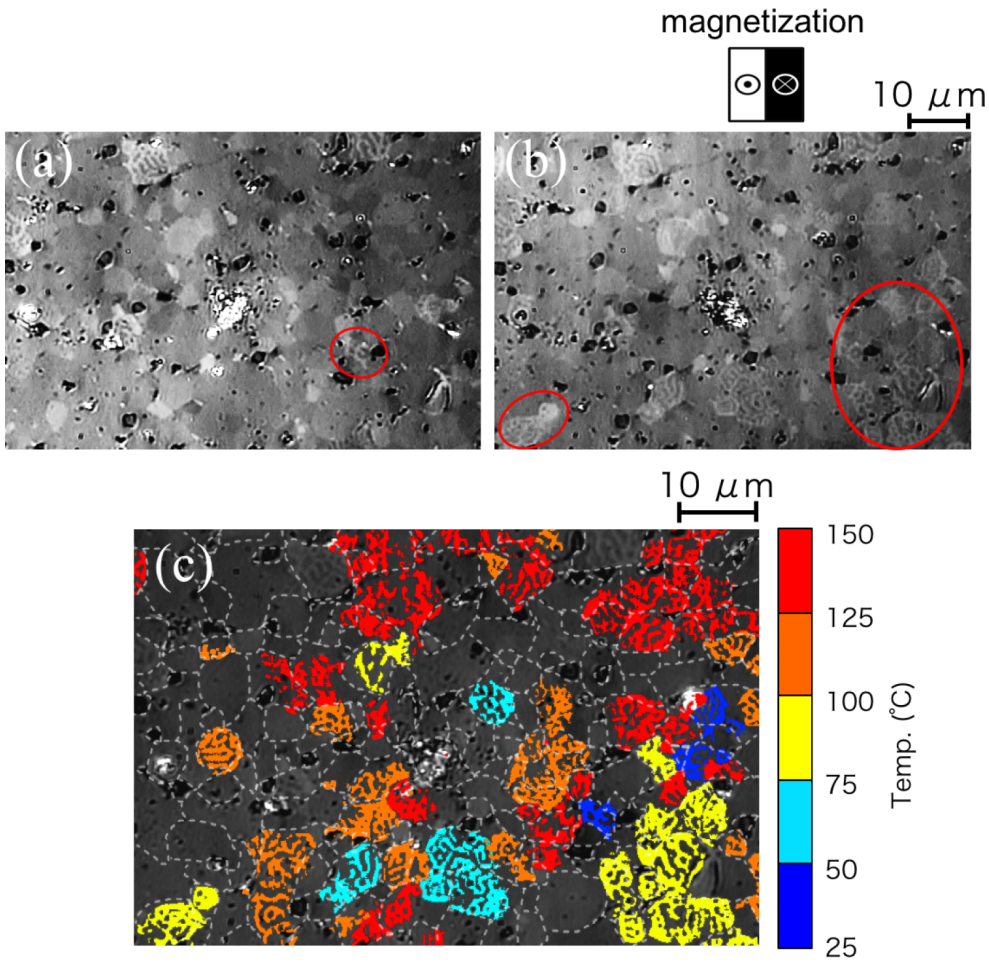

FIG. 2. Domain images of the Nd–Fe–B sintered magnet with a coercivity of $\mu_0 H_c = 1.25$ T at (a) 35 °C and (b) 90 °C, and (c) processed images indicating the magnetization-reversal area at each temperature.

120 °C, simultaneous magnetization reversal occurred in several adjacent grains beyond the grain boundaries, as indicated by the solid-line ellipse in Fig. 3(b). Figure 3(c) shows the processed domain image indicating the magnetization-reversal area for each temperature at 25 °C increments. The simultaneous magnetization reversal in several grains occurred above 75 °C, the temperature at which the reversal occurred in the case of the magnet with a coercivity of $\mu_0 H_c = 1.25$ T.

Figure 4 shows domain images of the Dy-added Nd–Fe–B sintered magnet with a coercivity of $\mu_0 H_c = 2.05$ T. Some demagnetized grains could be observed before heating, and the first magnetization reversal occurred after 35 °C heating, as indicated by the solid-line ellipse in Fig. 4(a), This reversal occurred at a lower temperature than that at which the reversal occurred for the magnet with a coercivity of $\mu_0 H_c = 1.69$ T. At 120 °C, simultaneous magnetization reversal occurred in several adjacent grains beyond the grain boundaries, as indicated by the solid-line ellipse in Fig. 4(b). Simultaneous magnetization reversal in a few grains was observed by increasing the temperature up to 150 °C, as shown in Fig. 4(c). However, the number of grains affected by the simultaneous magnetization reversal for the magnet with $\mu_0 H_c = 2.05$ T was lower than that of grains affected by the reversal for the other magnets with $\mu_0 H_c = 1.25$ and 1.69 T.

Thus, the temperature at which we observed the first nucleation of the reversal domains was not dependent on the coercivity of the magnets in the observation area of approximately 80 μm × 60 μm. The data indicate that the domain observation in the area was too local for statistical observation of the thermal demagnetization.

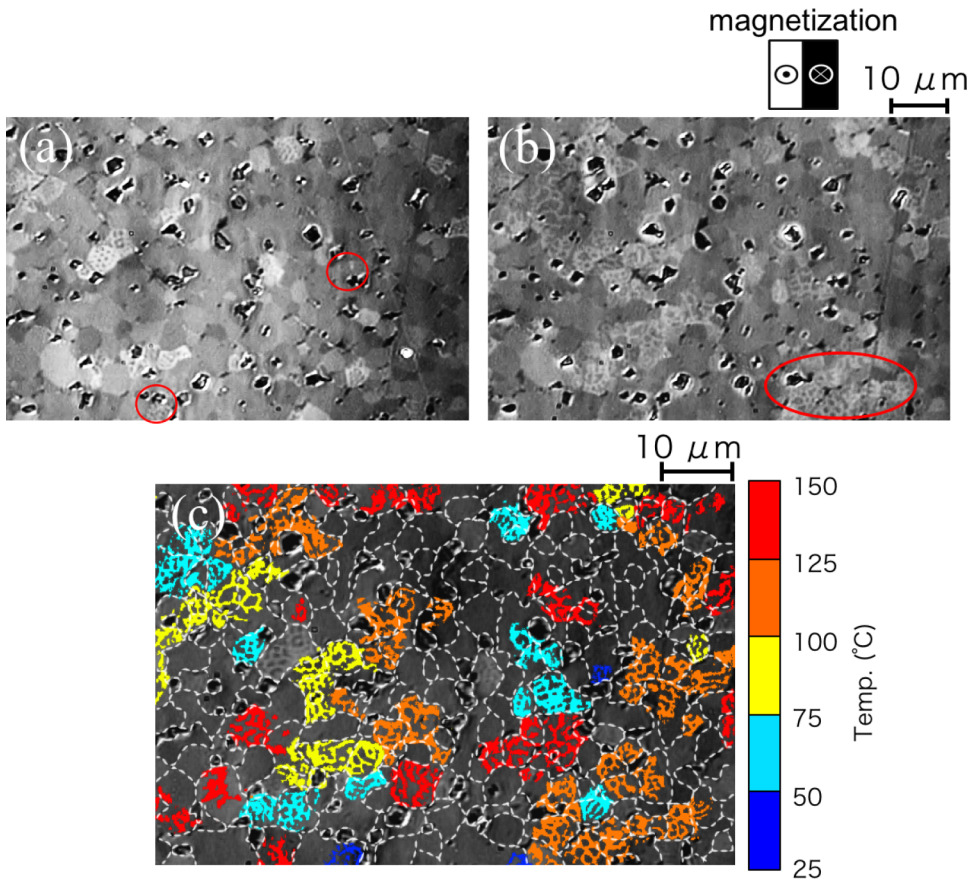

FIG. 3. Domain images of the Nd–Fe–B sintered magnet with a coercivity of $\mu_0 H_c = 1.69$ T at (a) 55 °C and (b) 120 °C, and (c) processed images indicating the magnetization-reversal area at each temperature.

B. Results of wide-field magnetic domain observation

To statistically analyze the thermal demagnetization, we increased the observation area to nine screens measuring approximately 240 μm × 180 μm. Figure 5 shows the image-processed domain image indicating the magnetization-reversal area of the magnet with a coercivity of $\mu_0 H_c = 1.25$ T at each 25 °C temperature increment.

The simultaneous magnetization reversal in approximately a hundred neighboring grains occurred from 75 °C to 100 °C, as shown in the lower-right corner in Fig. 5. We found that the thermal demagnetization easily occurred beyond the grain boundaries, and the reversal involved approximately a hundred grains in the low-coercivity Dy-free magnet with a coercivity of $\mu_0 H_c = 1.25$ T. Although the simultaneous magnetization reversal occurred at approximately 100 °C in the other two magnets with high coercivity, as shown in Figs. 6 and 7, the number of the neighboring grains that we observed with simultaneous reversal was small, ranging between several and 10 grains. It is important to note that the extent of the simultaneous reversal decreased in the Dy-added high-coercivity magnets with $\mu_0 H_c = 1.69$ and 2.05 T.

C. Calculation of demagnetizing ratio

Based on the observation results, we calculated the demagnetizing ratio in each sample using the following equation:

$$\text{Demagnetizing ratio}(\%) = \frac{(\text{Magnetization reversal area}) \times 2}{(\text{Total area}) - (\text{Defect area})} \times 100 \quad (1)$$

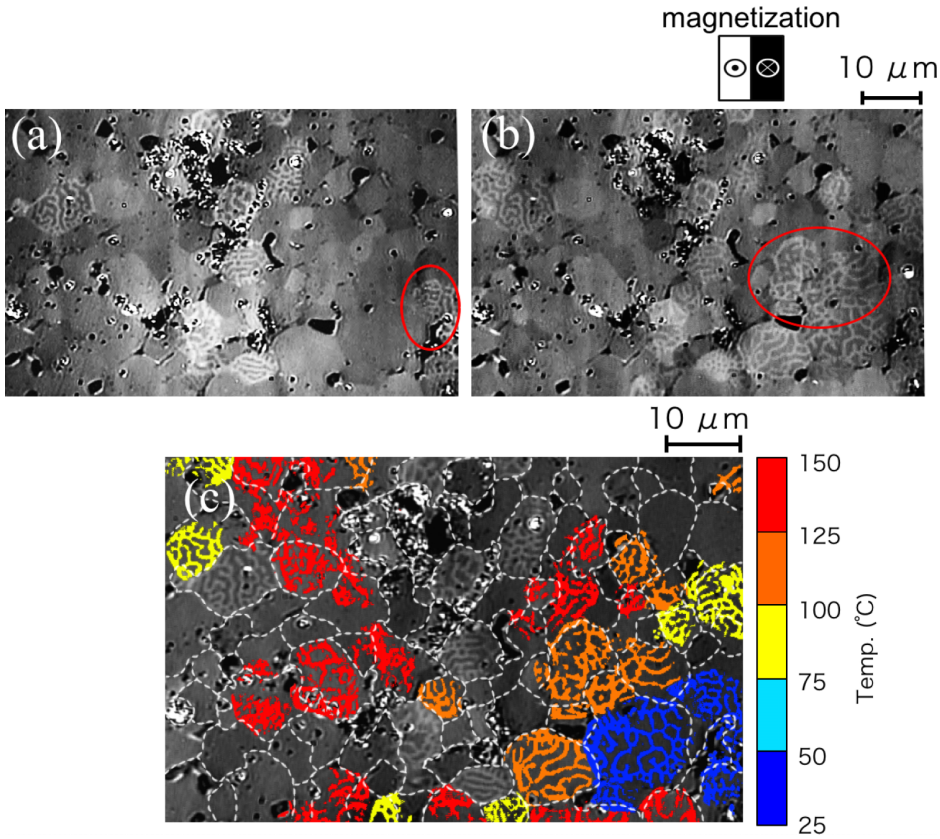

FIG. 4. Domain images of the Nd–Fe–B sintered magnet with a coercivity of $\mu_0 H_c = 2.05$ T at (a) 35 °C and (b) 120 °C, and (c) processed images indicating the magnetization-reversal area at each temperature.

In this equation, the ratio of the magnetization-reversal area to the total area, excluding the defect area, is multiplied by 2 to define the full demagnetization state as the demagnetizing ratio of 100%. The demagnetizing ratios after heating each magnet to 150 °C were 74.4% ($\mu_0 H_c$ = 1.25 T), 68.7% ($\mu_0 H_c$ = 1.69 T), and 67.8% ($\mu_0 H_c$ = 2.05 T). The demagnetizing ratios decreased with an increase in the coercivity of the magnets.

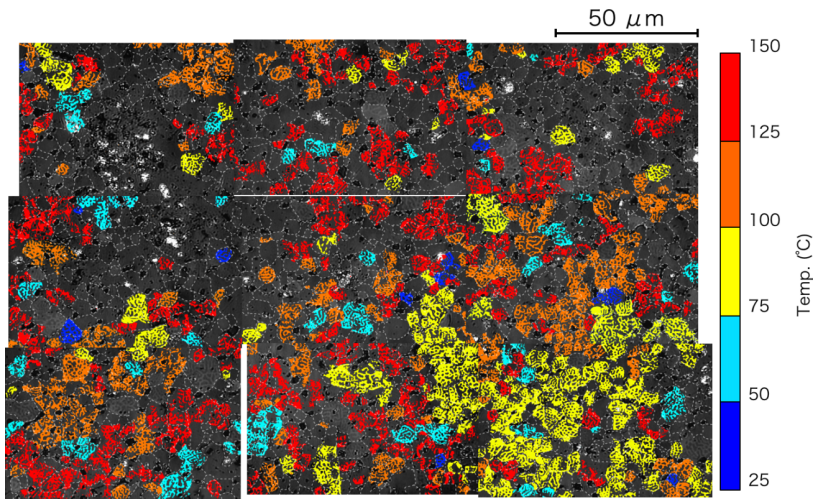

FIG. 5. Processed image of domains indicating the area of thermal demagnetization of the magnet with a coercivity of $\mu_0 H_c = 1.25$ T.

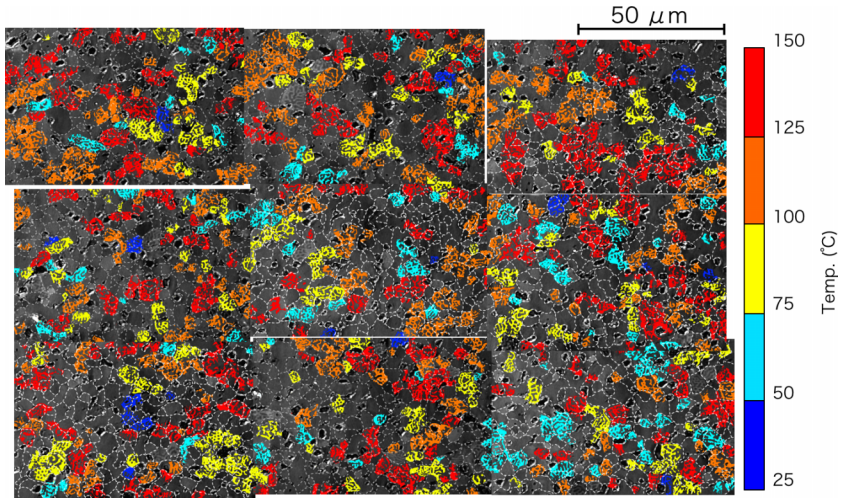

FIG. 6. Processed image of domains indicating the area of thermal demagnetization of the magnet with a coercivity of $\mu_0 H_c = 1.69$ T.

Figure 8 shows the dependence of the demagnetizing ratio on temperature. The demagnetizing ratio of the magnets with a coercivity of $\mu_0 H_c = 1.69$ and 2.05 T, respectively, increased with temperature, whereas that of the magnet with a coercivity of $\mu_0 H_c = 1.25$ T showed repetitions of sudden increases and stable situations. The demagnetization ratio precipitously increased at approximately 90 °C, following which it remained stable between 95 °C and 110 °C. Then, a sudden increase occurred at 110 °C, then it leveled off again between 110 °C and 125 °C.

Figure 9 shows the demagnetizing ratio at each temperature at 5 °C increments. As shown in the figure, high thermal demagnetization occurred at 90, 95, 115, and 130 °C in the magnet with a coercivity of $\mu_0 H_c = 1.25$ T. The high thermal demagnetization was caused by the propagation of magnetization reversal to the hundred adjacent grains, as shown in Fig. 5. The data indicate that the magnetic interaction beyond grain boundaries among the grains in the Dy-free low-coercivity magnet induced the high thermal demagnetization and affected thermal stability. On the other hand, the demagnetizing ratio of the magnet with a coercivity of $\mu_0 H_c = 2.05$ T above 100 °C was approximately 5% at each temperature. The precipitous increase in the demagnetizing ratio was not

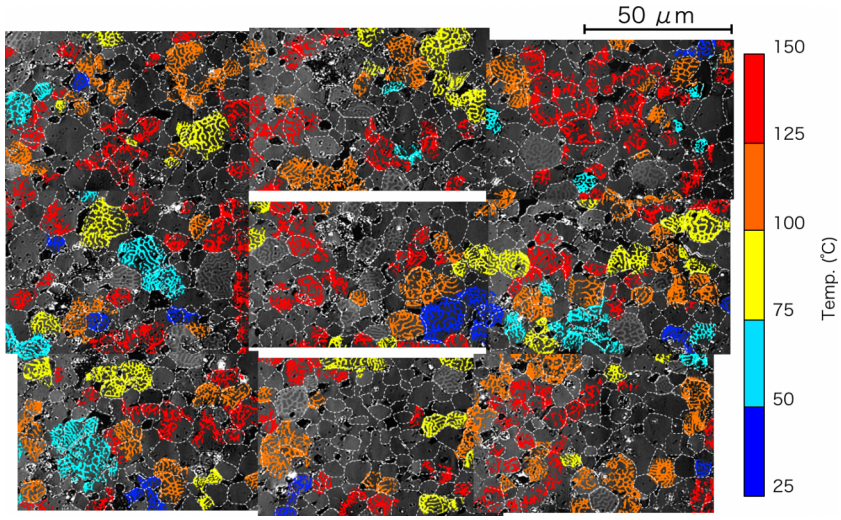

FIG. 7. Processed image of domains indicating the area of thermal demagnetization of the magnet with a coercivity of $\mu_0 H_c = 2.05$ T.

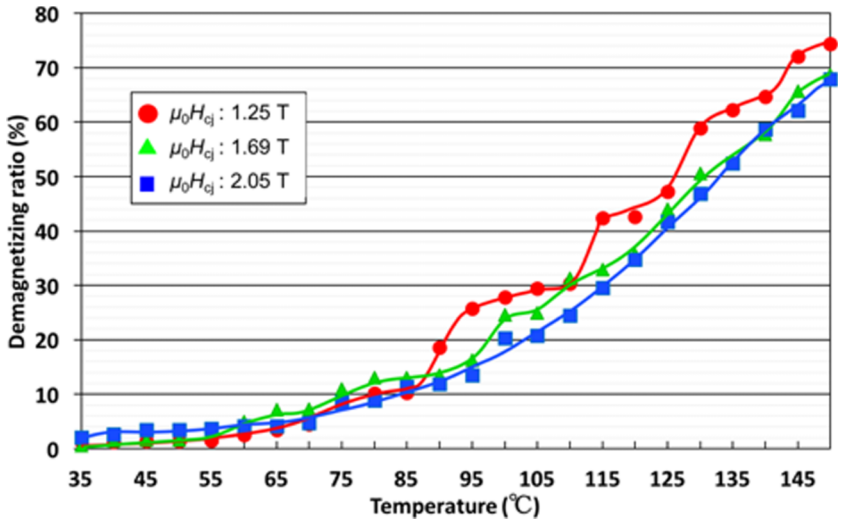

FIG. 8. The dependence of the demagnetizing ratio on temperature.

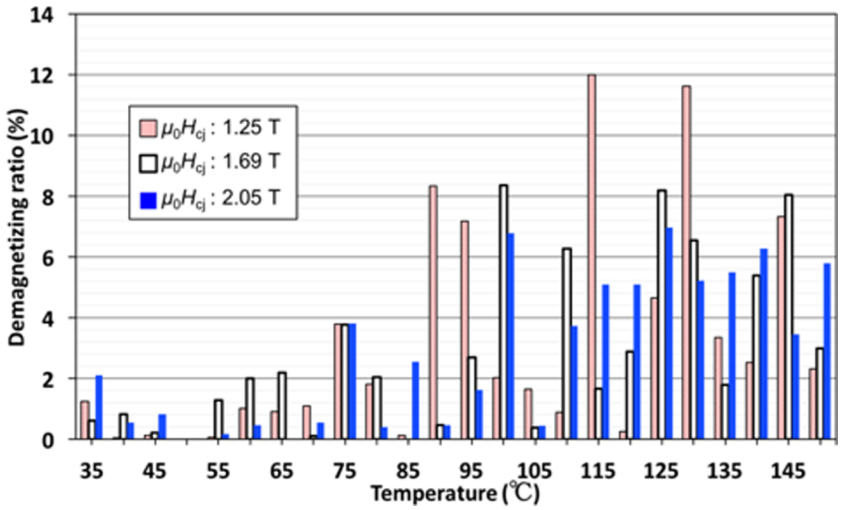

FIG. 9. The demagnetizing ratio at each temperature in 5 °C increments.

observed in the case of the Dy-added high-coercivity magnet. We found that the addition of Dy induced high thermal stability by eliminating simultaneous thermal demagnetization of a hundred neighboring grains because of the magnetic interaction among the grains.

IV. CONCLUSION

In the present study, using a Kerr microscope, we clearly observed the thermal demagnetization behavior of Nd–Fe–B sintered magnets when they were heated uniformly at elevated temperatures up to 150 °C. We found that simultaneous magnetization reversal in a hundred adjacent grains occurred because of the magnetic interaction beyond grain boundaries among grains in the Dy-free low-coercivity magnet at 90 °C. The simultaneous reversal in a hundred grains did not occur in the Dy-added high-coercivity magnets, and the demagnetizing ratio steadily increased with temperature. We found that the addition of Dy induced high thermal stability by eliminating the simultaneous thermal demagnetization, which was caused by the magnetic interaction among the grains. In our future research, it will be necessary to use domain observation to investigate the relationship between the magnetic interaction among grains and the thermal demagnetization

behavior of coercivity-enhanced magnets prepared using Dy or metal eutectic alloy diffusion techniques.[7,8] In addition, it will be necessary to investigate the relationship between the grain size and demagnetization process.

[1] S. Hirosawa, T. Nishiuchi, N. Nozawa, T. Ohkubo, K. Hono, H. Sepehri- Amin, M. Takezawa, J. Yamasaki, S. Yamanuro, T. Tanaka, M. Okano, and K. Sumiyama, in *Proceedings of the 21st Workshop on Rare-Earth Permanent Magnets and their Applications*, *Bled, Slovania* (2010), p. 187.
[2] S. Sugimoto, J. Jpn. Soc. Powder Powder Metall. **57**, 395 (2010).
[3] D. Li and K. J. Strnat, J. Appl. Phys. **57**, 4143 (1985).
[4] M. Takezawa, T. Shimada, S. Kondo, S. Mimura, Y. Morimoto, T. Hidaka, and J. Yamasaki, J. Appl. Phys. **101**, 09K106 (2007).
[5] M. Takezawa, H. Ogimoto, Y. Kimura, and Y. Morimoto, J. Appl. Phys. **115**, 17A733 (2014).
[6] M. Takezawa, Y. Kimura, Y. Morimoto, and J. Yamasaki, IEEE Trans. Magn. **49**, 3262 (2013).
[7] H. Nakamura, K. Hirota, M. Shimao, T. Minowa, and M. Honshima, IEEE Trans. Magn. **41**, 3844 (2005).
[8] H. Sepehri-Amin, T. Ohkubo, T. Nishiuchi, S. Hirosawa, and K. Hono, Scripta Materialia **63**, 1124 (2010).